

## Supporting Information

### **Light-Induced Synthesis of Clean-Surface PdPt@Pt Core-shell Nanoparticles with Excellent Electrocatalytic Activity**

**Tao Wang, Rong Yang, Shenshen Ouyang, Haibo Shi, and Sheng Wang\***

*\*e-mail: wangsheng571@hotmail.com*

*Key Laboratory of Advanced Textile Materials and Manufacturing Technology, Ministry of Education, Zhejiang Sci-Tech University, Hangzhou 310018, P. R. China.*

*E-mail: wangsheng571@hotmail.com*

#### **Table of Contents**

- S1. Experimental information
- S2. Formation mechanism of Pt seed nanoparticles under UV light irradiation.
- S3. XRD data of PdPt@Pt core-shell nanoparticles.
- S4. N<sub>2</sub> adsorption-desorption isotherm and pore size distributions of the samples.
- S5. Table 1. Binding energy and composition of PdPt@Pt core-shell nanoparticles measured from XPS, EDX and Figure S4.
- S6. Morphological evolution of Pd nanoparticles under UV light irradiation.
- S7. Morphological evolution of Pt nanoparticles under UV light irradiation.
- S8. HRTEM images of PdPt@Pt core-shell nanoparticles.
- S9. Morphological of PdPt@Pt core-shell nanoparticles collected at 5h and 6h.
- S10. Explanation on the choice of Pd seeds as core and Pt as shell and effects of light intensity.
- S11. Table 2. Data for the electrooxidation of CH<sub>3</sub>OH catalysed by the catalyst samples
- S12. Table 3. Comparison of the mass activities of Pd-Pt bimetallic catalysts for the MOR.

## S1. Experimental information

### Chemicals

Chloroplatinic acid ( $\text{H}_2\text{PtCl}_6 \cdot 6\text{H}_2\text{O}$ ) and sodium tetrachloropalladate ( $\text{Na}_2\text{PdCl}_4$ ) were purchased from Aladdin Reagents. Poly(vinylpyrrolidone) (PVP,  $M_w = 58000$ ), cetyltrimethylammonium bromide (CTAB), methanol ( $\geq 99.9$  wt%), ethanol ( $\geq 99.7$  wt%) and  $\text{HClO}_4$  ( $\approx 70$ -72 wt%) were commercially available from the Shanghai Chemical Reagent Co. Ltd. Nafion (5 wt%) was purchased from Sigma-Aldrich. Commercial Pt black and Pt/C catalysts (with 60% platinum loading) were purchased from Johnson Matthey Company.

### Photoreaction instrument

A photoreaction instrument (Nanjing Xujiang Co., Ltd) was used in this study and the schematic details are depicted in Figure S1. An ultrahigh-pressure Hg lamp (500 W, UV light between 315 and 400 nm) was located in the centre of the reactor along the axis and was protected by a water-cooled quartz jacket. At the bottom of the reactor, a magnetic stirrer was used to achieve effective dispersion through mechanical agitation. A circular test tube rack was inserted into the thermostatic bath to hold the Pyrex glass tubes. Thus, the UV light was illuminated the glass tube and ensured that the photoreaction occurred uniformly and completely. A magnetic stirrer stirred at 700 rpm to maintain vigorous agitation.

In this study, light intensity was set at 10000 Lux (approximately 1/10 of the normal intensity), which is beneficial to the dispersion and stability of nanoparticles (The explanation on the choice of Pd seeds as core and Pt as shell and effects of light intensity can be found in S9). The light intensity was detected using a UV light meter (UV-340A). Both the ultra-high-pressure Hg lamp and the reaction tube were maintained at a reaction temperature of  $25 \pm 1^\circ\text{C}$  by circulating cool water.

The reaction was finished in a single reaction tube. The second step was performed simply by injecting a proper amount of Pt precursor into the reaction tube. The obtained product could be used immediately without washing.

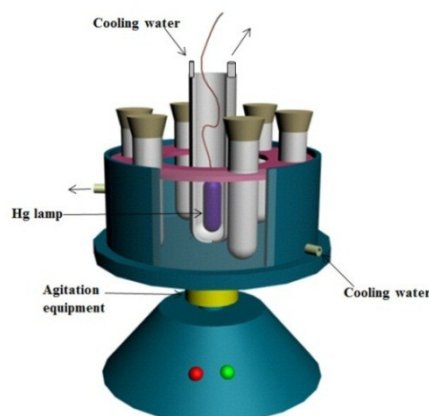


**Figure S1.** Schematic illustration of the photoreaction instrument.

### **Synthesis of Pd seed nanoparticles**

Photoreduction of Pd seed nanoparticles was performed by adding  $\text{Na}_2\text{PdCl}_4$  (0.2 mM) to a 50% v/v methanol/ $\text{H}_2\text{O}$  solution in a Pyrex tube. After  $\text{N}_2$  bubbling for 10 min to remove the dissolved  $\text{O}_2$ , the mixture solution was sealed and irradiated with a 500 W high-pressure mercury lamp (the intensity of the UV light was adjusted to 10000 Lux by covering the mercury lamp with a stainless-steel mesh) for 5 h while stirring the solution vigorously (700 rpm).

### **Synthesis of PdPt@Pt core-shell nanoparticles**

After a certain amount of Pt precursor (in this work, the molar ratio of  $\text{Na}_2\text{PdCl}_4$  to  $\text{H}_2\text{PtCl}_6$  was 1:2) was injected into the solution under agitation, the mixture was irradiated continuously for 4 h while stirring (700 rpm). The obtained sample was centrifuged and dried at about  $60^\circ\text{C}$  for 12 h.

### **Preparation of structure-directing agent adsorbed PdPt@Pt core-shell nanoparticles**

In this work, the effects of structure-directing agents were investigated by applying two common structure-directing agents, CTAB and PVP ( $M_w = 58000$ ). First, the clean-surface PdPt@Pt core-shell nanoparticles were immersed in a CTAB/PVP solution (the concentration was set at 0.03 M) for 12 h. After collecting and washing the nanoparticles with ethanol and water several times, the CTAB/PVP-adsorbed catalysts were obtained.

### **Electrochemical measurements**

All the electrochemical measurements were performed on the electrocatalysts using a CHI660E electrochemical workstation. A platinum wire and  $\text{Hg}/\text{Hg}_2\text{Cl}_2$  (saturated KCl) were used as the counter and reference electrodes, respectively. A glassy carbon electrode (GCE, 3 mm diameter) was polished to a mirror finish (with 1.0, 0.3, and 0.05 mm alumina powder, respectively) and thoroughly cleaned. To prepare the working electrode, 2  $\mu\text{L}$  of Nafion (0.05%)-ethanol suspensions of the catalyst sample or commercial catalyst was dropped on the surface of a GCE, respectively. The Pt loading of the catalysts is  $20 \mu\text{g}/\text{cm}^2$ .

Methanol oxidation reaction (MOR) measurements were carried out in acidic media. The MOR was performed in an  $\text{HClO}_4$  (0.5 M) aqueous solution containing methanol (0.5 M) at a potential from 0 to 1.0 V. Chronoamperometry was carried out in  $\text{HClO}_4$  (0.5 M) and methanol (0.5 M) at 0.5 V vs. SCE. All the measurements were performed at room temperature and the CV was performed at a scan rate of  $50 \text{ mV s}^{-1}$ .

### **Characterisation methods**

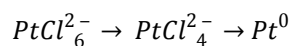
Transmission electron microscopy (TEM) samples were prepared by suspending the nanoparticles in ethanol and then casting onto a holey, carbon-coated Cu grid. High-resolution TEM images were obtained using a JEM-2010 (HR) instrument operating at 200 kV. Energy

dispersive X-ray analysis (EDX, Inca Energy-200) was used to investigate the sample compositions. X-ray diffraction (XRD) patterns were obtained on a D/MAX-RB X-ray diffractometer (D/Max-2550pc) using Cu-K $\alpha$  radiation at a scan rate ( $2\theta$ ) of 0.05° s $^{-1}$ , and the patterns were used to determine the phase structure of the obtained samples. The accelerating voltage and the applied current were 15 kV and 20 mA, respectively. S<sub>BET</sub> and BJH pore-size distributions were determined using a Micromeritics Tristar 3000. High-angle annular dark-field scanning TEM (HAADF-STEM) characterisations were performed with a FEI Technai G2 F30 S-Twin transmission electron microscope operating at 200 kV. The metal contents of the catalysts were measured using ICP-OES (Optima 2100 DV; Perkin Elmer). X-ray photoelectron spectrum (XPS) analysis was performed on a Thermo Scientific K-Alpha system.

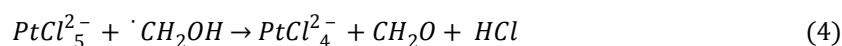
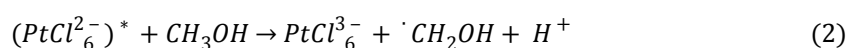
## S2. Formation mechanism of noble metal nanoparticles under UV light irradiation

According to a reference paper on the growth of noble metal nanoparticles,<sup>1</sup> UV light acts as an energy trigger in the photochemical reaction, which excites a metal precursor to form activated species that react with methanol.

Here, we use a Pt precursor as an example. The irradiation of  $\text{PtCl}_6^{2-}$  in an aqueous alcoholic solution generates Pt nanoparticles through the formation of  $\text{Pt}^0$ .



Upon UV light irradiation, the excited  $\text{Pt}^{4+}$  is reduced by the alcohols to generate  $\text{Pt}^{3+}$  (Eq. 2). The oxidised alcohols become the oxidative radicals, which subsequently reduce the  $\text{Pt}^{3+}$  species to  $\text{Pt}^{2+}$  (Eq. 5). In addition, the disproportionation forms  $\text{Pt}^{2+}$  (Eq. 6) through the formation of  $\text{Pt}^{3+}$  species



The reaction leads to the formation of  $\text{Pt}^0$ , followed by the reduction of the  $\text{Pt}^{2+}$  ionic species. The  $\text{Pt}^0$ – $\text{Pt}^0$  bond then forms, resulting in the development of nanoparticles through the association of  $\text{Pt}^0$ – $\text{Pt}^0$ .

1. M. Harada and H. Einaga, *Langmuir*, 2006, **22**, 2371-2377.

## S3. XRD data of PdPt@Pt core-shell nanoparticles

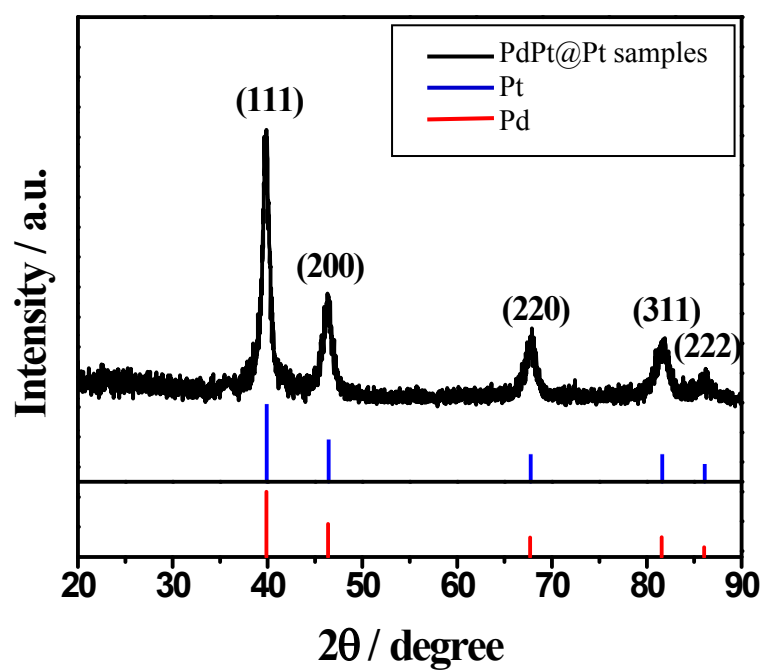
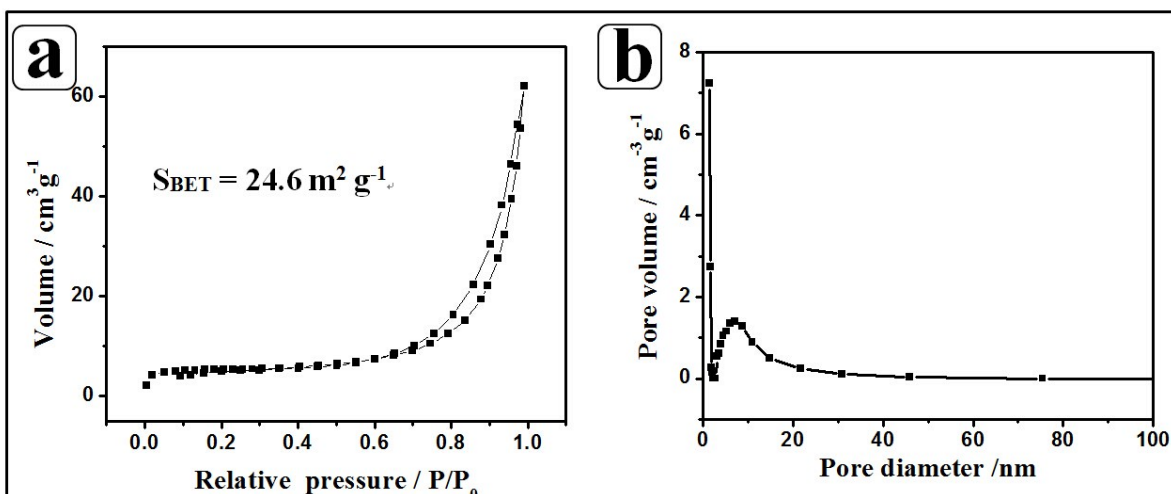


Figure S2. XRD patterns of PdPt@Pt core-shell nanoparticles.

S4. N<sub>2</sub> adsorption-desorption isotherm and pore size distributions of the sample



**Figure S3.** (a) N<sub>2</sub> adsorption-desorption isotherm of the PdPt@Pt core-shell nanoparticles and (b) pore-size distribution curve obtained from the BJH method.

**S5. Table 1.** Binding energy and the composition of the samples measured by XPS and EDX

sample	Pt 4f <sub>7/2</sub> BE(eV)		Pd 3d <sub>5/2</sub> BE(eV)		Pd:Pt <sup>c</sup>	Pd:Pt <sup>d</sup>	Pd:Pt <sup>e</sup>
	Pt <sup>0</sup>	Pt <sup>2+</sup>	Pd <sup>0</sup>	Pd <sup>2+</sup>			
Pd/Pt (1:2)	72.1 (85.1%) <sup>a</sup>	75.4 (14.9%) <sup>a</sup>	336.2 (90.7%) <sup>b</sup>	338.1 (9.3%) <sup>b</sup>	5.8:94.2	37:63	34.8:65.2

<sup>a</sup> Relative % of the Pt<sup>0</sup> and Pt<sup>2+</sup> species. <sup>b</sup> Relative % of the Pd<sup>0</sup> and Pd<sup>2+</sup> species.

<sup>c</sup> Surface atomic ratio calculated according to XPS analysis using peak areas normalised on the basis of sensitivity factors.

<sup>d</sup> Atomic ratio obtained from the TEM-based EDX analysis.

<sup>e</sup> Result obtained from ICP-AES.

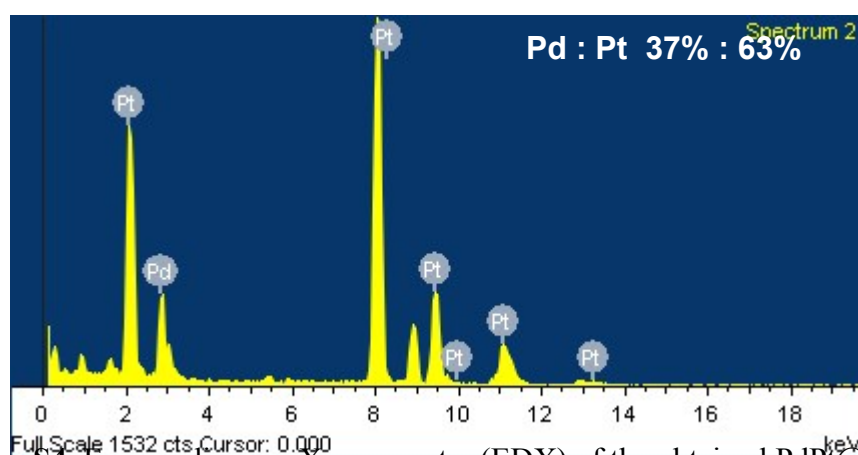


**Figure S4.** Energy-disperse X-ray spectra (EDX) of the obtained PdPt@Pt core-shell nanoparticles.

## S6. Morphological evolution of Pd nanoparticles under UV light irradiation



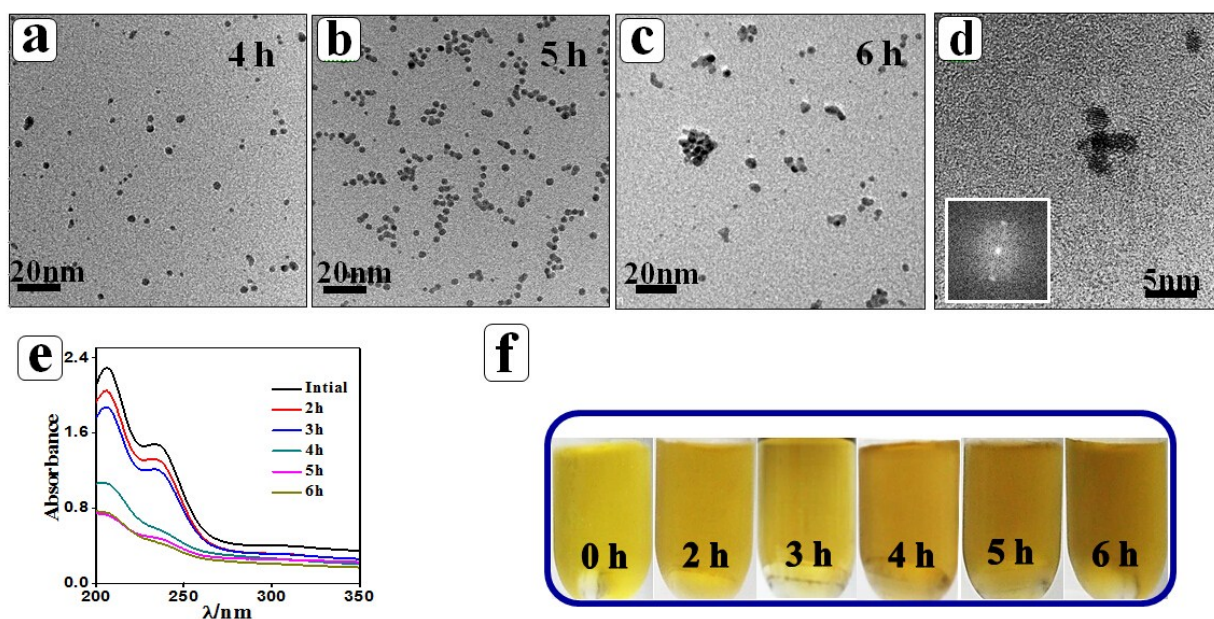


**Figure S5.** TEM images showing the morphological evolution of Pd nanoparticles at (a) 4 h (b) 5 h, and (c) 6 h. (d) High magnification TEM image of a single Pd aggregate (6 h) and its corresponding FFT pattern (inset). (e) Corresponding analysis by UV/vis spectroscopy of aliquots taken at different reaction times. (f) Photographs of colloidal suspensions taken at different reaction times.

The progression of the UV light-induced synthesis of Pd nanoparticles was monitored by UV/vis absorption spectroscopy at different reaction times. According to a reference paper, UV/vis spectra demonstrated the reduction of the Pd(IV) ions through the disappearance of two characteristic absorption peaks at 206 and 233 nm, which correspond to  $\text{Na}_2\text{PdCl}_4$ .<sup>1,2</sup>

1: S. Ghosh, S. Mondal, C. R. Raj, *J. Mater. Chem. A*, 2014, **2**, 2233-2239.

2: T. Harada, S. Ikeda, M. Miyazaki, T. Sakata, H. Mori, M. Matsumura, *Journal of Molecular Catalysis A: Chemical*, 2007, **268**, 59-64.

## S7. Morphological evolution of Pt nanoparticles under UV light irradiation

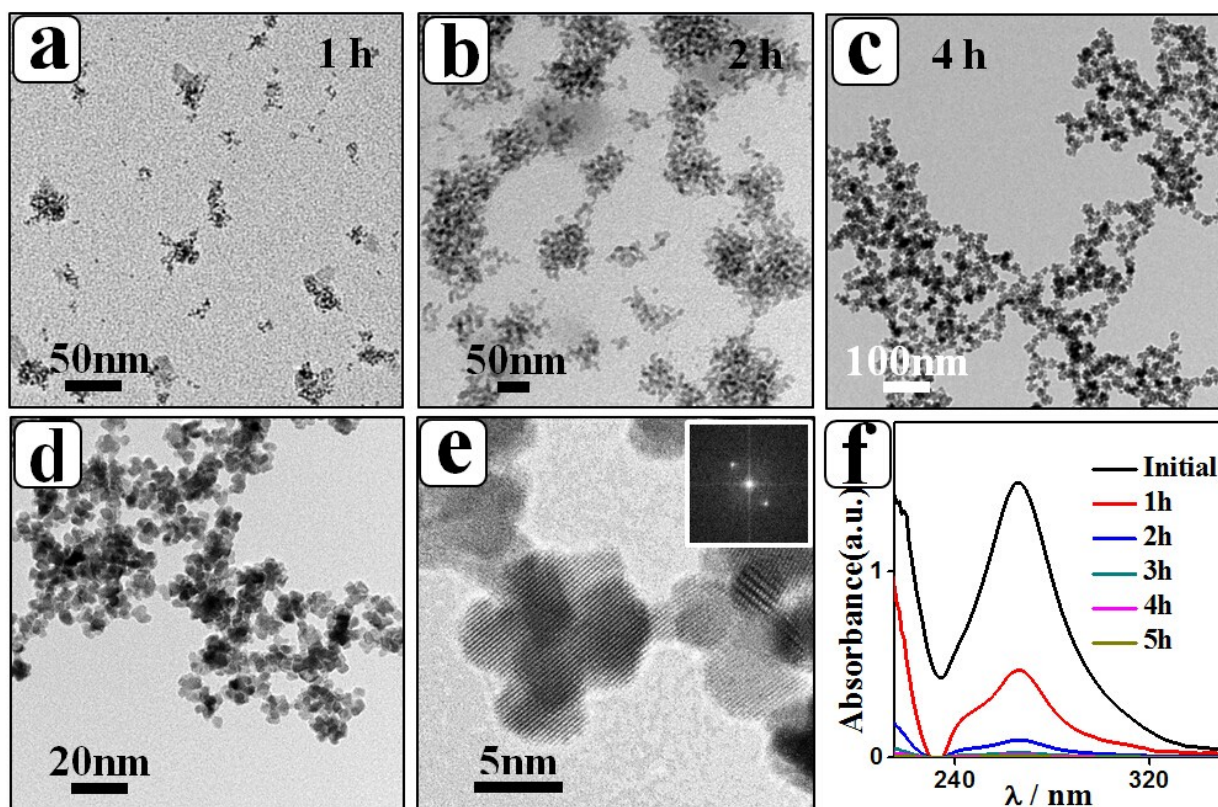


**Figure S6.** TEM images showing the morphological evolution of Pt nanoparticles at (a) 1 h, (b) 2 h, and (c) 4 h. (d), (e) High magnification TEM images of a single Pt nanobranched structure (4 h) and its corresponding FFT pattern (inset). (f) Corresponding analysis by UV/vis spectroscopy of aliquots taken at different reaction times.

The progression of the UV light-induced synthesis of Pt nanoparticles was monitored by UV/vis absorption spectroscopy at different reaction times. The relative concentration of the precursor solution was evaluated by assessing two characteristic absorption peaks of Pt complexes, centred at 201 and 265 nm, which correspond to  $\text{H}_2\text{PtCl}_6$ .<sup>1,2</sup> Upon increasing the reaction time, the Pt concentration gradually decreased. All Pt ions were completely consumed after 3 hours of reaction.

1: T. Nakamura, S. Ichihara, *T. Den, ECS Trans.*, 2007, **3**, 275.

2: Y. Shin, I-T. Bae, G. J. Exarhos, *Colloids and Surfaces A: Physicochem. Eng. Aspects* 2009, **348**, 191-195.

## S8. HRTEM images of PdPt@Pt core-shell nanoparticles



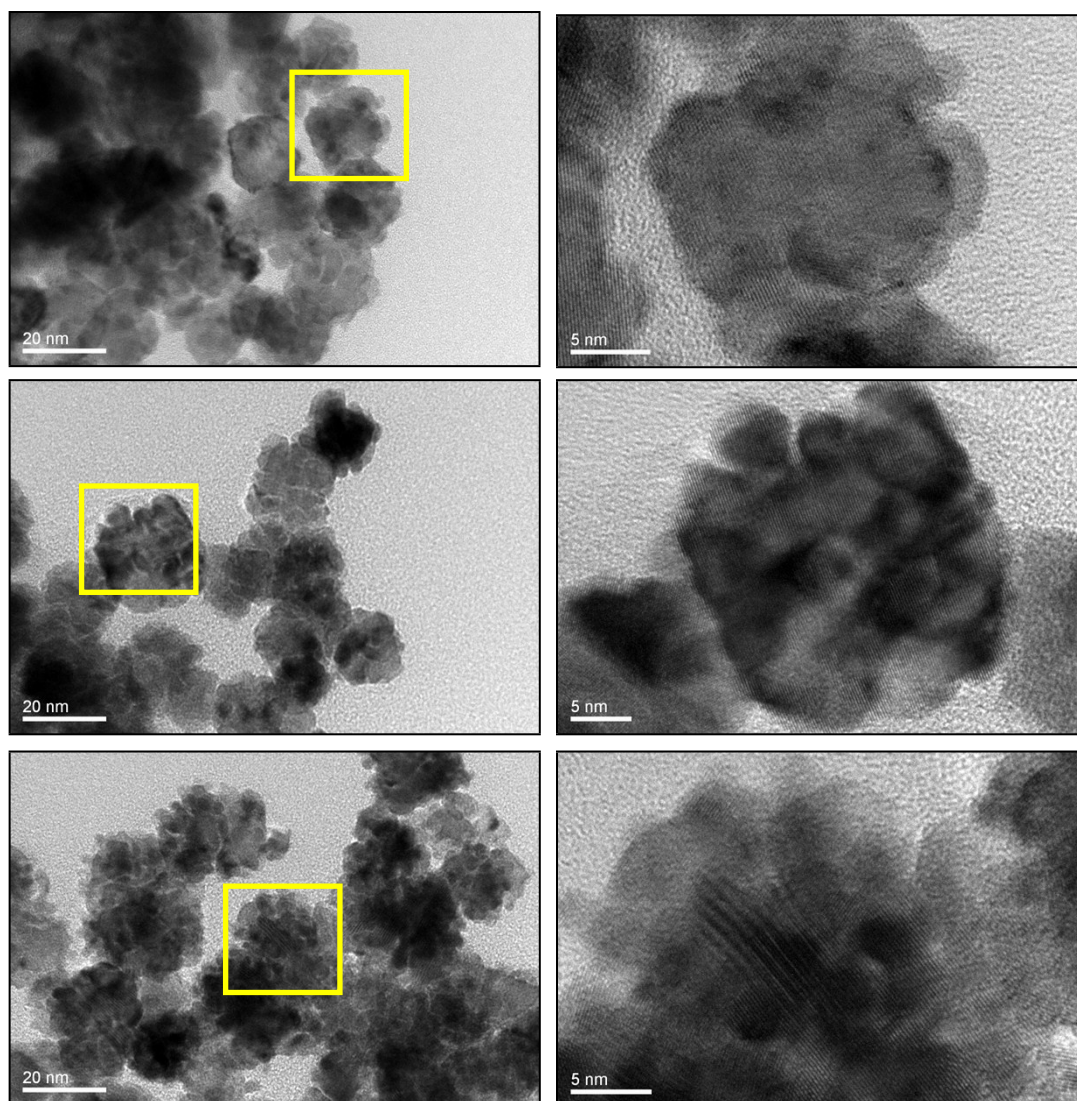


**Figure S7.** HRTEM images of PdPt@Pt core-shell nanoparticles.

**S9.** Morphological of PdPt@Pt core-shell nanoparticles collected at 5h and 6h.

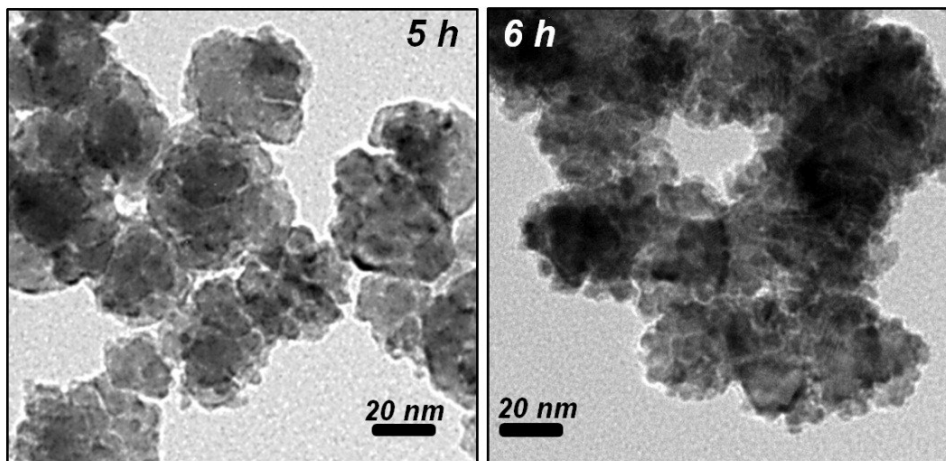


**Figure S8.** TEM images showing the morphological of PdPt@Pt nanoparticles obtained at (a) 5 h, (b) 6 h.

### S10. Explanation on the choice of Pd seeds as core and Pt as shell and effects of light intensity.

At the very beginning of the experiment, we have attempted a one-step process. However, under the experimental conditions, neither the product morphology (Figure S8) nor the electrocatalytic activity was satisfactory.

One possible explanation is that in the present experimental conditions, it takes much more time for the reduction of Pd than Pt (as mentioned above, according to the reduction potential of  $\text{PdCl}_4^{2-}/\text{Pd}$  (0.62 V) and  $\text{PtCl}_6^{2-}/\text{Pt}$  (0.725 V)). Therefore, many early formed Pt may aggregate and act as a core component, and most latter formed Pd will aggregate at the outside, which will waste efficient active component Pt and lead to the lower electrocatalytic activity.

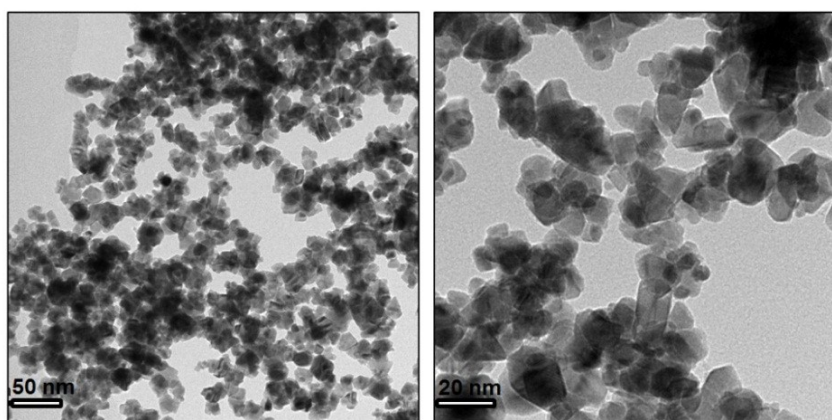


**Figure S9.** TEM images showing the morphological of sample nanoparticles obtained via a one-step process.

On the other hand, our investigation clearly indicates that in the synthesis of either Pt/Pd nanoparticles or PdPt@Pt nanoparticles, UV light, photoreducing agents, methanol and  $\text{N}_2$  are all indispensable.

- 1): Without UV illumination, reduction cannot occur at room temperature following only addition of methanol and metal precursor.
- 2): Conversely, without methanol, reduction cannot occur only by irradiation of the metal precursor solution.
- 3): As mentioned above, UV light acts as an energy trigger in the photochemical reaction, which excites the metal precursor to form activated species that react with methanol.
- 4): Light intensity accelerates the formation of the nanoparticles in our experimental system.

The following figure shows the effect of light intensity on the formation of Pt nanoparticles. When the light intensity was increased to 40000 Lux, macro-scale aggregation was obtained within an hour. Because the process was performed without structure-directing agents and

considering the morphology and stability of the final product, 10000 Lux was determined to be the optimal light intensity.

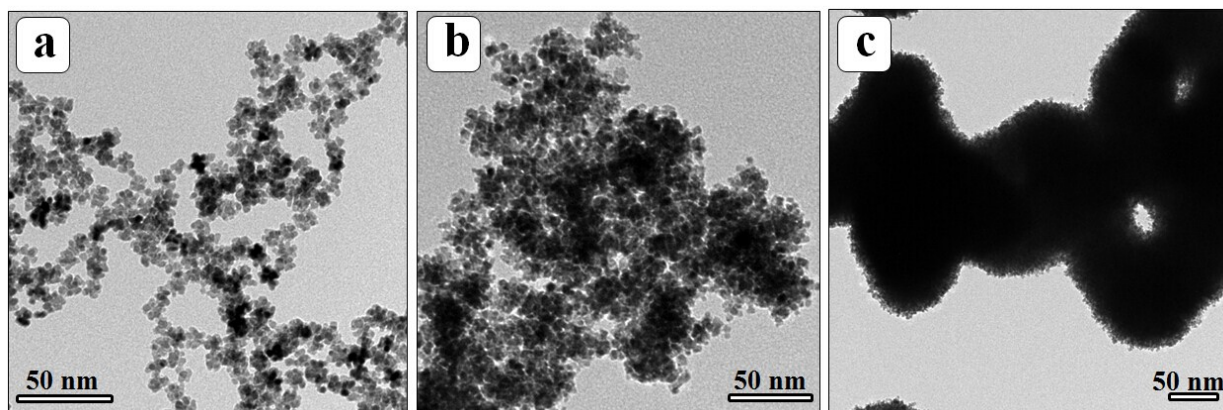


**Figure S10.** TEM images showing the morphological of Pt nanoparticles obtained at different light intensity (a) 10000 Lux, 4h; (b) 20000 Lux, 2h; (c) 40000 Lux, 1h.

**S11. Table 2.** Data for the electro-oxidation of CH<sub>3</sub>OH catalysed by the catalyst samples

Catalyst	Pt loading	ECSA	Mass activity	Specific activity
	[ $\mu\text{g}$ ]	[ $\text{m}^2\text{g}_{\text{Pt}}^{-1}$ ]	[ $\text{mA}\text{mg}_{\text{Pt}}^{-1}$ ]	[ $\text{mA}\text{cm}^{-2}$ ]
		<b>Acidic</b>	<b>media</b>	
Pt black	2.0	11.5	94.5	0.82
Pt/C	2.0	17.2	156.0	0.90
Pure Pt	4.0	16.9	365.0	2.17
nonoflowers PdPt@Pt	2.9	44.3	993.0	2.24
PdPt@Pt (CTAB)	2.9	17.3	242	1.40
PdPt@Pt (PVP)	2.9	7.1	148	2.08

**S12. Table 3.** Comparison of Pd@Pt core-shell catalysts for the MOR

Pd@Pt catalyst	Particle size (nm)	Acidic media			Reference
		ECSA	Pt/C	Pt Black	
<b>PdPt@Pt</b> (no structure-directing agent, reducing agent: CH <sub>3</sub> OH )	<b>20</b>	<b>44.3</b>	<b>6.4</b>	<b>10.5</b>	<b>This work</b>
Pd@Pt (no structure-directing agent, reducing agent: NH <sub>2</sub> OH·HCl)	9.45/8.23	52.04		4.4	1
Pd@Pt (no structure-directing agent, reducing agent: ascorbic acid)	36	13.9	2.8		2
Pd@Pt (CTAB)	30-40			6.0	3
mesoporous Pd@Pt (Pluronic F127)	45			4.2	4
Pd@Pt nanocage (Pluronic F127)	42			5.3	5

1. H. Wu, H. Li, Y. Zhai, X. Xu, and Y. Jin, *Adv. Mater.*, 2012, **24**, 1594-1597.
2. Y. Kim, Y. W. Lee, M. Kim, and S. W. Han, *Chem. Eur. J.*, 2014, **20**, 7901-7905.
3. H. Zhang, Y. Yin, Y. Hu, C. Li, P. Wu, S. Wei and C. Cai. *J. Phys. Chem. C.*, 2010, **114**, 11861-11867.
4. H. Atae-Esfahani, M. Imura and Y. Yamauchi. *Angew. Chem. Int. Ed.*, 2013, **52**, 13611-13615.
5. L. Wang and Y. Yamauchi. *J. Am. Chem. Soc.*, 2013, **135**, 16762-16765.